THE JOURNAL OF BIOLOGICAL CHEMISTRY
Vol. 276, No. 32, Issue of August 10, pp. 29671–29680, 2001

Printed in U.S.A.

Effects of Diabetes Insipidus Mutations on Neurophysin Folding and Function*

Received for publication, April 19, 2001, and in revised form, June 5, 2001
Published, JBC Papers in Press, June 6, 2001, DOI 10/1074/jbc.M103477200

Sharon Eubanks‡, Tam L. Nguyen‡, Ruba Deeb‡, Art Villafania‡, Ayna Alfadhli§, and Esther Breslow‡¶

From the ‡Department of Biochemistry, Weill Medical College of Cornell University, New York, New York 10021 and the §Department of Chemistry, Portland State University, Portland, Oregon 97207-0751

Mechanisms underlying the pathogenicity of diabetes insipidus mutations were probed by studying their effects on the properties of bovine oxytocin-related neurophysin. The mutations G17V, ΔE47, G57S, G57R, and C67STOP were each shown to have structural consequences that would diminish the conformational stability and folding efficiency of the precursors in which they were incorporated, and factors contributing to the origins of these property changes were identified. Effects of the mutations on dimerization of the folded proteins were similarly analyzed. The projected relative impact of the above mutations on precursor folding properties qualitatively parallels the reported relative severity of their effects on the biological handling of the human vasopressin precursor, but quantitative differences between thermodynamic effects and biological impact are noted and explored. The sole mutation for which no clear thermodynamic basis was found for its pathogenicity was 87STOP, suggesting that the region of the precursor deleted by this mutation plays a role in targeting independent from effects on folding, or participates in stabilizing interactions unique to the human vasopressin precursor.

The hormone vasopressin is synthesized as part of a larger precursor that contains the vasopressin sequence at its amino terminus, followed by that of the disulfide-rich protein neurophysin (NP)[1] and a carboxyl-terminal glycopeptide known as copeptin (Ref. 1 and reviewed in Ref. 2). Oxytocin biosynthesis is similar (3), with the exception that the precursor lacks the copeptin segment, the function of which is unclear (4). The NP components of the two precursors (^{VP}NP) and (^{Oxy}NP) are highly homologous; the two bovine neurophysins have almost identical properties *in vitro*, including similar affinities for each of the two hormones (*e.g.* Ref. 2). Following processing, which cleaves the hormones from NP, the mature hormones remain noncovalently bound to NP by forces basically analogous to those pre-existing within the precursor, leading to analogous NP self-association properties (5). The structure of NP, the nature of the noncovalent interactions between hormones and NP, and the effects of these interactions on NP properties have been extensively investigated in solution (*e.g.* Ref. 2) and by crystallographic analysis (6, 7). Moreover, the central role of NP in vasopressin elaboration has become evident by the demonstration that familial neurogenic diabetes insipidus (FNDI), an autosomal dominant disease characterized by vasopressin deficiency, appears most frequently to be due to mutations in NP (*e.g.* Refs. 8 and 9) accompanied by loss of the proper targeting of the hormone to regulated neurosecretory granules (*e.g.* Refs. 10 and 11); retention of the mutated precursor in the endoplasmic reticulum is generally considered the cause of the ultimate death of the affected neurons (10).

Many of the mutations involved in diabetes insipidus can be predicted, on the basis of what is already known, to exert their effects by directly or indirectly interfering with NP folding and/or dimerization (*e.g.* Refs. 12 and 13). Protein targeting to regulated neurosecretory granules is thought to depend at least in part on self-association, although the nature of the requisite self-association process is not well defined (reviewed in Ref. 14). In the case of oxytocin and vasopressin precursors, the self-association arises from the self-association properties of their NP segments. The central element of this self-association is the dimer, the formation of which occurs through specific β-sheet interactions between folded NP subunits (6, 7) and is strongly enhanced by the binding of hormone or related peptides to the binding site (15). The efficiency of NP folding is in turn critically linked to the correct but metastable (16) pairing of its 7 disulfides and depends, with one known exception (17), on the ability of the protein to bind hormone and thereby provide the necessary thermodynamic stability to drive formation of the correct disulfides to completion. Thus, mutations (*e.g.* Ref. 9) that interfere with disulfide formation by deleting or adding half-Cys residues, or that alter binding site residues, can be expected to affect adversely both folding and targeting.

However, there are a number of FNDI mutations for which the molecular mechanisms underlying their biological effects are ambiguous and therefore have the potential to provide new information on the relationship between structure and function in this system. These include mutations in residues involved neither in binding nor dimerization, such as those in external β-turns or in the 55–60-loop region that connects the two NP domains, or a premature STOP mutation that deletes both copeptin and the disordered (6, 7) carboxyl-terminal NP tail (9). They also include mutations affecting more clearly essential

* This work was supported by National Institutes of Health Grant GM-17528 from NIH. The costs of publication of this article were defrayed in part by the payment of page charges. This article must therefore be hereby marked "*advertisement*" in accordance with 18 U.S.C. Section 1734 solely to indicate this fact.

¶ To whom correspondence should be addressed: Dept. of Biochemistry, Weill Medical College of Cornell University, 1300 York Ave., New York, NY 10021. Tel.: 212-746-6428; Fax: 212-746-8875; E-mail: ebreslow@mail.med.cornell.edu.

[1] The abbreviations used are: NP, neurophysin; ^{VP}NP, vasopressin-related neurophysin; ^{Oxy}NP, oxytocin-related neurophysin; FNDI, familial neurogenic diabetes insipidus; BNP-I, bovine oxytocin-related NP; BNP-II, bovine vasopressin-related NP; WT, wild type; Phe-Tyr-NH_2, L-phenylalanyl-L-tyrosine amide; Phe-PheNH_2; L-phenylalanyl-L-phenylalanine amide; Abu-TyrNH_2, L-α-amino-butyryl-L-tyrosine amide; turn AG mutant, mutant of BNP-I containing an Ala-Gly insert between residues 17 and 18 of WT; ER, endoplasmic reticulum; Mes, 2-(*N*-morpholino)ethanesulfonic acid; HPLC, high pressure liquid chromatography.

```
                                10                  20                  30
Human   A M S D L E L R Q C L P C G P G G K G R C F G P S I C C A D E L G C F
BNP-II  ----------------------------------------------------------------G----------
BNP-I   ----V L------D V----T------------------------------------------ ---G----------

                40                  50                  60                  70
Human   V G T A E A L R C Q E E N Y L P S P C Q S G Q K A C G S G G R C A A F
BNP-II  ------------------------------------------------------------P ----------A
BNP-I   ------------------------------------------------------------P---------- ---------A

                            80                  90
Human   G V C C N D E S C V T E P E C R E G[    ] F H R R A
BNP-II  --- I---------------------------------------- IVG---- P ----- V
BNP-I   ----I-------S P D G--- H E D---A---D P E  A A --- S  Q
```

FIG. 1. **Sequence of human ^{VP}NP compared with that of bovine ^{VP}NP (BNP-II) and bovine ^{Oxy}NP (BNP-I).** Data are from Ref. 19. Note that the sequence of BNP-I and its mutants used in this study terminate at Ser-92 (20).

residues. Accordingly, we have investigated the effects of these mutations on NP physical-chemical properties. Mutations studied that do not involve obviously essential residues are G57S and G57R in the inter-domain loop (8, 9), G17V in the first β-turn (18), and 87STOP near the carboxyl terminus (9). Additionally, we investigated the C67STOP mutation, which deletes most of the second domain of the protein, together with half of the subunit interface and one cysteine, and the ΔE47 mutation that deletes the critical binding site residue Glu-47 (*e.g.* 9), located in the 3,10 helix of the protein.

The effects of these mutations were principally investigated by introducing them into bovine ^{Oxy}NP and in one case into the oxytocin precursor, for both of which we have developed an expression system. This takes advantage of the strong homology in structure and function between ^{Oxy}NP and ^{VP}NP within and among different mammalian species (2, 19). Fig. 1 compares the amino acid sequences of bovine ^{Oxy}NP (BNP-I), bovine ^{VP}NP (BNP-II), and human ^{VP}NP. With the exception of the carboxyl-terminal tail, for which no function is known, there are only 4 amino acid differences between bovine and human ^{VP}NP, and none involve residues at the hormone-binding or dimerization sites. Also, with the exception of the carboxyl-terminal tail, which is eliminated when the protein is terminated with residue 86, all the mutated residues are strictly conserved. Therefore, it seems reasonable to expect that the similarity in behavior between bovine ^{Oxy}NP and bovine ^{VP}NP will be paralleled by a similarity between bovine ^{Oxy}NP and human ^{VP}NP; a single exception to this may be evident in these studies. It is also relevant that the present study emphasizes the effects of mutation on mature NP, as opposed to the NP segment of the precursor. We selected this route because of the inefficiency associated with the *in vitro* folding of the wild type precursor (20), which contrasts with the efficiency of folding the wild type processed protein using added dipeptide to drive the folding process (16, 21). In the single case in which the effects of mutation on both the processed protein and precursor are compared, the same effect is seen. A few studies of the effects of chemical or enzymatic modification of the two bovine NPs are also presented. Fig. 2 is a diagram of NP structure, including its disulfide pairs, that shows the positions of the different mutations investigated.

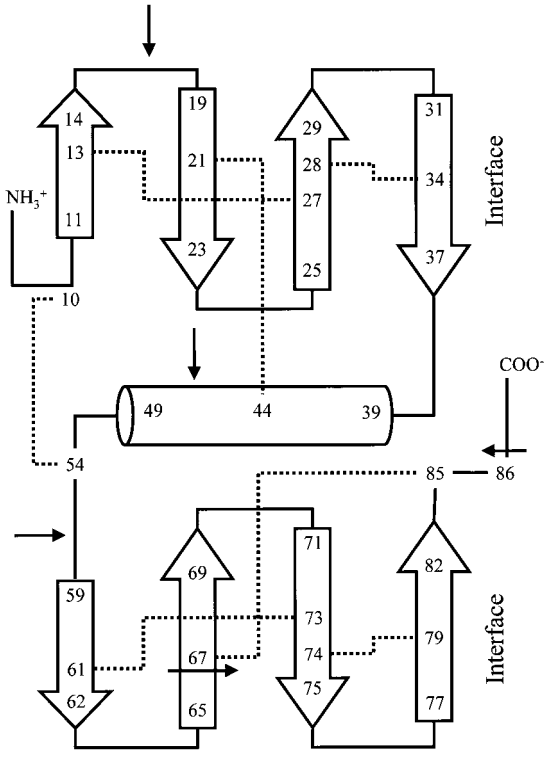

FIG. 2. **Diagram of the structure of BNP-II showing the position of the mutations introduced into BNP-I.** The *dotted lines* show the disulfide connectivities.

MATERIALS AND METHODS

Preparation of Wild Type and Recombinant Proteins—BNP-I and -II, isolated from bovine posterior pituitary lobes as described previously (22, 23), and affinity-purified (24), were used for all studies of the wild type (WT) mature proteins. The preparation of recombinant WT mature BNP-I and oxytocin precursor and mutagenesis of wild type cDNA have been described previously (17, 20). The recombinant mature mutant proteins in the present study were expressed in *Escherichia coli*, folded at pH 8.0 in the presence of β-mercaptoethanol and 10 mM Phe-Tyr-NH_2, and purified by affinity chromatography as described for the recombinant mature WT protein (17). A large fraction of the protein so prepared is covalently damaged prior to folding (17, 20), and the remaining protein folds with variable efficiency depending on its structure (see below). The covalent structures of mutants were confirmed by DNA sequencing of the plasmids from which they were prepared and by mass spectrometry. With proteins that fold efficiently, the binding-competent and binding-incompetent proteins are distinguished by clear differences in mass, reflecting the covalent damage of the binding-incompetent protein (20). This was not the case for several of the mutants, indicating the inability of undamaged protein to fold efficiently ("Results").

None of the ΔE47 mutant was retained by the affinity column after folding (as expected because of its incomplete binding site), but because of CD evidence of folded product within the binding-incompetent fractions (245 nm positive ellipticity), this mutant was further fractionated by reverse phase HPLC using a Vydac C_{18} column, 10× 250 mm, and a gradient from 100% solution A (25% CH_3CN, 40 mM ammonium acetate) to 100% solution B (80% CH_3CN, 40 mM ammonium acetate) at

150 min. A sharp peak at 13 min gave a CD spectrum characteristic of folded protein and was used for further analysis. The same HPLC protocol was applied to the C67STOP mutant, but only a diffuse peak eluting approximately between 14 and 24 min was obtained ("Results").

The G57S mutation was also introduced into the full-length oxytocin precursor. The precursor was folded, and the folded precursor was purified essentially as described previously for the WT precursor (20).

Folding Efficiencies of Recombinant Proteins—Although purified WT BNP-I refolds from the reduced state with ~90% efficiency under our folding conditions (21), the yield from the initial folding reaction of folded recombinant WT protein, or of its stable mutants, is considerably lower than 90% and is somewhat variable, reflecting the covalently damaged protein formed during expression. Nonetheless, the folding efficiencies of the G57S, G57R, and P87STOP mutants were within the experimental range of that of WT and other stable proteins, whereas yields of the ΔE47 mutant and turn AG insertion mutant were reduced by factors of ~50 and 80% respectively. The folding efficiency of the G17V mutant was significantly lower than that of the turn AG mutant, but was too low for accurate estimates. Note that the theoretical folding efficiency of the WT protein under the conditions used here can be calculated to be ~95%, indicating an equilibrium heavily in favor of the folded form. Therefore, only relatively large reductions in stability should be manifest as a significant reduction in yield.

Chemical and Enzymatic Modification of Wild Type Protein—Succinylated BNP-I was prepared from native BNP-I as described elsewhere (25). Following succinylation, protein retarded by the affinity column is succinylated at its two Lys residues and randomly succinylated at Ser residues exclusive of Ser-56, whereas protein not retarded by the affinity column differs from the retarded fraction by its succinylation at Ser-56 (25).

For preparation of BNP-I with a specific internal clip after Lys-18, 13 mg of native BNP-I was digested with 3 units of endoproteinase Lys-C (Sigma) for 24 h at 37 °C in 0.5 ml of 0.1 M NH_4HCO_3 buffer, pH 9. Residual native protein was separated from the cleaved protein by affinity chromatography (15), the cleaved protein not binding to the affinity column. On native polyacrylamide gel electrophoresis at pH 9.5, the non-binding protein gave two bands, a major product (≥80% of the protein) migrating with the expected additional negative charge relative to the native protein and a minor band with the same mobility as the native protein. Automated Edman sequencing confirmed cleavage after Lys-18 but gave no evidence of any undigested protein. Two controls were run in order to determine whether factors other than cleavage after Lys-18 could account for the altered conformational properties (see "Results") of the digested protein. No significant effect on conformation was noted if the native protein was subjected to enzymatic digestion conditions in the absence of enzyme or if protein succinylated at its two Lys residues was subjected to enzymatic digestion conditions in the presence of enzyme.

Des-1–6 BNP-II was prepared as described earlier (26). The des-1–6,des-87–95 protein was prepared from the purified des-1–6 derivative by limited digestion with trypsin (1% by weight) at room temperature in 0.16 mM KCl, 50 mM Tris buffer, pH 8.2. Digestion was monitored by non-denaturing polyacrylamide gel electrophoresis at pH 9.5 and was terminated by snap-freezing aliquots at −80 °C. The crude modified protein was purified by HPLC on a Vydac C18 reverse phase column using a gradient from time 0 (25% acetonitrile, 0.1% trifluoroacetic acid in water) to 40 min (35% acetonitrile, 0.1% trifluoroacetic acid in water). The method separates the des-1–6,des-87–95 protein (retention time = 20 min) from des-1–6,des-93–95 protein (retention time = 22 min) and from most of the more completely digested protein; the latter is completely removed by a subsequent affinity chromatography (24) step. Binding fractions from affinity chromatography, representing the des-1–6,des-87–95 protein, were dialyzed against water and lyophilized. Purity and identity were confirmed by native polyacrylamide gel electrophoresis and amino acid analysis. Relative to the initial native BNP-II used, the yield of the final des-1–6,des-87–95 protein was ~4%.

Determination of Peptide Binding Constants and Dimerization Constants—Peptide binding constants were determined by CD using the mononitrated derivatives of the different mutants and binding methodology described elsewhere (*e.g.* Ref. 27); the peptides used were Phe-Tyr-NH_2 or Abu-Tyr-NH_2, depending on availability. Dimerization constants were determined from one-dimensional proton NMR spectra obtained in D_2O as described previously (17), measuring the intensity ratio at different protein concentrations of signals at ~6.4 and 6.2 ppm representing dimer and monomer, respectively; the validity of the use of these signals in the mutants was verified by demonstrating that the calculated dimerization constants were independent of protein concentration.

Stability Measurements—Stabilities to denaturation by guanidine HCl were determined by one or both of the two methods. In the conventional method, applied earlier to this system, CD spectra were obtained by a constant concentration of protein in different concentrations of guanidine HCl (17, 20). In the second method (28), carefully weighed quantities of solid guanidine HCl are added serially to a sample of protein; the guanidine concentration is calculated from the weight of guanidine added and known dilution factors. This method, which was used for many preparations because of its smaller protein requirement, is intrinsically less accurate, due in part to the concentration dependence of the stability of WT mature NP and many of its mutants (17). Nonetheless, good agreement between the two methods was seen where the two methods were applied to the same sample (Table I). Both methods assume a two-state denaturation system, and both typically have a reproducibility of better than 5%, although occasional exceptions are evident.

Other Methods—Most other methods have been described previously, *i.e.* determination of protein folding kinetics (16), NMR, CD (*e.g.* Refs. 16 and 20), mass spectrometry (20), amino acid analysis, and protein sequencing (*e.g.* Ref. 25). Protein modeling utilized the Swiss Protein Data Bank modeling system and the crystal structures of des-1–6 bovine NP-II in its unliganded state[2] and as its lysine vasopressin complex.[2]

RESULTS

Effects of the G57S and G57R Mutations—Gly-57 does not participate directly in either binding or dimerization (6, 7), and the G57S mutant folded with an efficiency within the range of the WT protein (see "Materials and Methods"). The near-ultraviolet CD spectrum of the affinity-purified G57S mutant (Fig. 3), which represents the contribution of NP disulfides, is identical to that of the WT protein (Fig. 3), consistent with a similarity in conformation. Note that this spectrum is very sensitive to NP folding; the 245-nm positive band is absent in misfolded protein, and the 280-nm negative band is reduced in intensity and shifted to shorter wavelengths (*e.g.* Ref. 29). One-dimensional NMR spectra were also largely similar to spectra of BNP-I, but significant differences were evident in the intensity ratio of monomer and dimer signals at ~6.2 and ~6.4 ppm at the same protein concentration (Fig. 4). Calculation of this ratio as a function of concentration indicated a dimerization constant 20–30% that of BNP-I (Table II). Surprisingly (*cf.* Ref. 17), the stability to guanidine denaturation was unaffected (Table I), suggesting that the reduced dimerization might reflect increased monomer stability. The peptide binding constant of the G57S mutant was also reduced by 20–30%, but as with the WT protein the binding affinity increased with protein concentration, signifying stronger binding by dimer than by monomer (Table III). NMR studies (not shown) confirmed the peptide-induced conversion of monomer to dimer. The effects of concentration on binding and of binding on dimerization are tentatively consistent with estimates of an ~10-fold higher binding constant to a dimer site than to a monomer site found for the WT protein (27), resulting in a 100-fold increase in dimerization constant in the bound state (30).

The reduction in binding constant by G57S is greater than can be accounted for by the reduction in its dimerization constant, *e.g.* the binding constant of G57S can be shown to only half that calculated for BNP-I when the two are compared at equivalent weight fractions of dimer as described for other mutants (17). This is particularly evident with the G57R mutant. The dimerization constant of this mutant is the same or slightly higher than that of the G57S mutant (Table II), but, at similar protein concentrations, its binding affinity for Abu-Tyr-NH_2 is ~1/4 that of the G57S mutant, and its binding affinity for Phe-Tyr-NH_2 is only 13% that of BNP-I (Table III). Again, the link between binding and dimerization is preserved in the

[2] C. K. Wu, B. Hu, J. P. Rose, Z.-J. Liu, T. L. Nguyen, C. Zheng, E. Breslow, and B. C. Wang, submitted for publication.

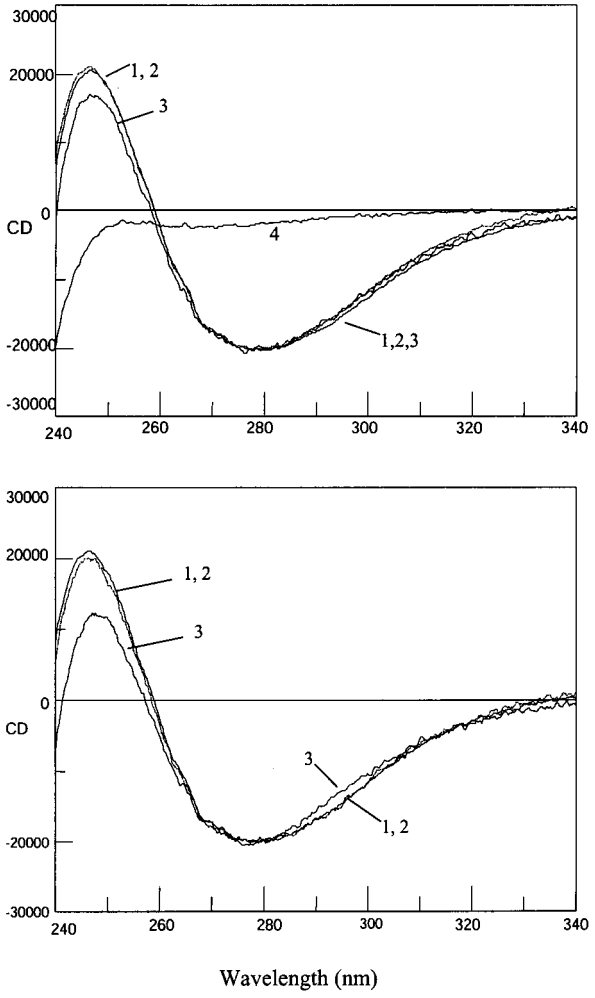

FIG. 3. **Near-ultraviolet CD spectra at neutral pH of the folded forms of WT BNP-I and of various mutants.** The spectrum of the C67STOP mutant is shown for comparison. *Top spectra, curve 1,* WT BNP-I; *curve 2,* G57S; *curve 3,* G57R; and *curve 4,* C67STOP. *Lower spectra, curve 1,* WT BNP-I; *curve 2,* P87STOP; and *curve 3,* ΔE47. Results are expressed as molar (not residue) ellipticities. To show differences in 245/280 nm ellipticity ratios, data for all mutants except C67STOP are normalized to a value of −20,000 at 280 nm, the ellipticity of the WT protein, although small differences among the mutants in absolute ellipticity might be present.

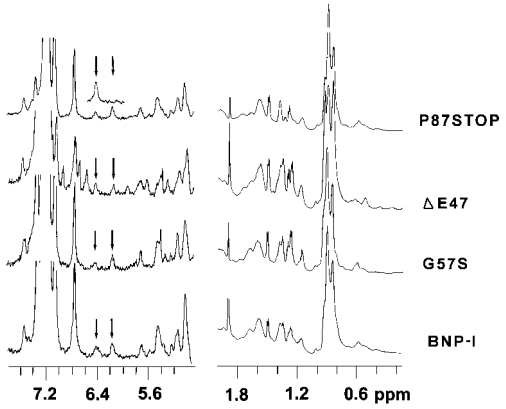

FIG. 4. **600 MHz proton NMR spectra of the correctly folded forms of WT BNP-I and of selected mutants in D_2O at a protein concentration of 0.3 mM, pH 6.2.** *Arrows* point to the α-proton signals at ~6.4 ppm (dimer) and 6.2 ppm (monomer) used to calculate dimerization constants. Signals upfield from 0.55 ppm and the small signal at ~1.0 ppm are also assigned to dimer. The partial spectrum above the full spectrum of the 87STOP mutant represents the same sample in the presence of 2 mM Phe-PheNH_2; the peptide has no signals in this region. The increase in the 6.4 ppm signal and disappearance of the 6.2 ppm signal show the ligand-induced increase in dimer content.

G57R mutant as judged by the dependence of its binding on concentration (Table III) and by NMR studies (not shown). Factors additional to reduced dimerization therefore operate to reduce the binding affinities of both mutants. The CD spectrum of the G57R mutant (Fig. 3) is slightly altered relative to that of the wild type protein in the unliganded state, raising the possibility that it has a slightly altered conformation. This is consistent with modeling studies (see "Materials and Methods") that suggest weak steric hindrance from Arg-57 in the unliganded state that becomes more pronounced in the liganded state. Modeling studies similarly suggest that the G57S mutation should introduce steric problems in the liganded state but significantly less so than the Arg-57 mutation; again, fewer problems are evident in the unbound state. The modeling results therefore provide an explanation for the binding affinity reductions in the two mutants that do not arise from the reduction in dimerization.

Because the effects of Gly-57 on dimerization suggested a modulating role in dimerization for the loop between the two domains, the effects on dimerization of succinylation of Ser-56 were also investigated. This modification was shown previously to lead to a large decrease in binding constant (25). Table II demonstrates a reduction in dimerization in the unliganded state by a factor of 2–3 when NP succinylated at Ser-56 is compared with protein similarly modified with the exception of Ser-56 (see "Materials and Methods").

Precursor stability depends strongly on the strength of interaction between hormone and NP segments (20); so the effects of Gly-57 mutation on binding predict a diminution in the stability of the oxytocin precursor containing such mutations (17, 20). The G57S mutation was accordingly incorporated into the precursor (see "Materials and Methods"), and its effect on stability was evaluated. Previous studies of the WT precursor had demonstrated a pH-dependent dissociation of the internal interactions between the oxytocin and NP segments of the wild type precursor with a CD midpoint near pH 10 (20). The clearest CD indicator of this transition (least influenced by tyrosine ionization (20)) was the change in the ratio of ellipticity at 291 nm to that at 280 nm, which occurs with a midpoint of 9.7 in the WT precursor (20). The neutral pH spectrum of the G57S precursor (Fig. 5) was similar to that of the wild type (*cf.* Ref. 20) and similarly exhibited a pH-dependent transition characteristic of internal hormone-protein dissociation. However, the CD midpoint was shifted downward to pH 9.25 in the G57S precursor (Fig. 5), indicating (20) a 0.6 kcal/mol weaker free energy of internal bonding between hormone and NP than in the WT precursor.

The difference between the WT and G57S precursors in the strength of interaction between hormone and NP was also manifest by a difference in stability to guanidine denaturation (Fig. 5). Denaturation midpoints were at 3.85 M guanidine and 4.25 M guanidine for the G57S and WT precursors, respectively, and did not significantly change with protein concentration over the range studied. Comparison of the stabilities of the WT and mutant precursors (Table I) calculated from their individual denaturation profiles indicated a lower stability of the mutant by 0.3–0.4 kcal/mol. However, the intrinsic uncertainty in the absolute value of ΔG^0 for each protein (see Table I) leads to still greater uncertainty in the differences calculated in this manner. Since the shapes of the denaturation profiles of both proteins are essentially identical (Fig. 5), and the derived values of m for the two proteins are within the experimental error of these measurements (Table I), we also estimated the stabil-

TABLE I
Stabilities to guanidine HCl denaturation of wild type and mutant proteins

Studies were conducted at pH 6.0 in 0.1 M ammonium acetate unless otherwise noted. A and B represent the denaturation method used, where A is that used in earlier NP studies (17, 20), and B involves addition of solid guanidine HCl (see "Materials and Methods"). The value m is the slope of the guanidine denaturation free energy curve (40). Data are reported to two significant figures ± S.E. of readings at 247 and 250 nm unless otherwise indicated.

Protein	Concentration	m	$-\Delta G^0$	
			A	B
	mM	*kcal mol* M^{-1}	*kcal/mol*	
BNP-I	0.04	1.1	3.1 ± 0.1[a]	
BNP-I	0.05	1.2 (±0.0)		2.9 (±0.03)
WT precursor	0.04	1.6	6.8 ± 0.4[a]	
WT precursor	0.02	1.6 (±0.06)		7.0 (±0.2)
WT precursor	0.05	1.7 (±0.03)		7.4 (±0.06)
G57S	0.05	1.1 (±0.07)	3.1 (±0.1)	
G57S precursor	0.025	1.7 (±0.09)		6.6 (±0.15)
G57S precursor	0.05	1.8 (±0.04)		7.1 (±0.15)
ΔE47	0.06	1.0 (0 ± 0.1)		2.7 (±0.2)
P87Stop	0.05	1.1 (±0.07)		3.0 (±0.05)
BNP-II[b]	0.1	0.94 (±0.35)		2.5 (±0.07)
Des-1–6,des-87–95 BNP-II[b]	0.1	0.84 (0 ± 0.06)		2.5 (±0.05)
BNP-II[c]	0.1	0.64 (±0.1)	2.1 (±0)	
Des-1–6 BNP-II[c]	0.1	0.68 (±0.04)	2.3 (±0.4)	

[a] Data are those previously reported (20).
[b] Data were obtained at pH 8 in 0.1 M Tris-HCl buffer.
[c] Data are averages of results at 252 and 280 nm.

TABLE II
Effects of selected mutations on neurophysin dimerization in D_2O at pH 6.2

The estimated error in dimerization constants is ±20%.

Protein	Dimerization K (M^{-1})	
	No salt	+ 0.1 M ammonium acetate
BNP-I	3.2×10^3	1.0×10^4
G57S	1.0×10^3	1.8×10^3
G57R	1.0×10^3	2.8×10^3
BNP-I succinylated at Ser-56	1.4×10^3	5×10^3
BNP-I, succinylated, Ser-56-free	4.2×10^3	1.2×10^4
P87Stop	1.5×10^3	
ΔE47	3.3×10^3	
BNP-II	5.4×10^3	
Des-1–6, BNP-II	2.4×10^4	
Des-1–6,des-87–95 BNP-II	6.5×10^3	

ity difference between the two proteins from the difference in their denaturation midpoints (0.4 M), assuming the same value of m for each (1.7), and the relationship (Equation 1),

$$\Delta\Delta G^0 = 0.4 \text{ M } (1.7 \text{ kcal mol}^{-1} \text{ M}^{-1}) = 0.68 \text{ kcal/mol} \qquad \text{(Eq. 1)}$$

By either consideration, the lower stability of the G57S precursor calculated from the guanidine data is reasonably consistent with that estimated from the pH data and therefore appears primarily to arise from weaker internal NP-oxytocin interactions.

Effects of the G17V Mutation and Related Studies of the Role of the 14–18 Turn—Gly-17 is part of the turn connecting the first two strands of β-sheet (Fig. 2). Mutation to Val yielded very low quantities of binding-competent protein (see "Materials and Methods"). Mass spectrometry indicated that both the binding-competent protein and a large fraction of the non-binding protein had the correct mass, suggesting that much of the non-binding protein was not covalently damaged (see "Materials and Methods") but reflected an unfavorable folding equilibrium. This was confirmed by resubjecting the non-binding protein to folding conditions, followed by the same workup as given to the original folding mixture. Upon affinity chromatography, a similar percentage of protein was found in the binding fraction as found following the initial folding reaction (data not shown).

TABLE III
Effects of mutations and modifications on neurophysin binding affinities

Studies were conducted at pH 6.2 and 25 °C in 0.1 M ammonium acetate, containing 20 mM Mes buffer. Values in parentheses are the protein concentrations at which binding constants were determined. Relative binding constants (last column) are reported to one significant figure and represent the ratio of the experimental constant to that of BNP-I (or BNP-II where applicable) at the same protein concentration; where two values are given, the first is for the Abu peptide. Binding constants for the WT proteins, when not experimentally determined at a given protein concentration, were calculated from the known concentration dependence of binding (27).

Protein	Experimental binding K		Relative K values
	Abu-Tyr-NH_2	Phe-Tyr-NH_2	
	M^{-1}		
BNP-I	1700 (0.1 mM)	14,000 (0.2 mM)	1.0, 1.0
		6,000 (0.02 mM)	1.0, 1.0
G57S	420 (0.08 mM)		0.3
	160 (0.02 mM)		0.2
G57R	100 (0.07 mM)	1400 (0.07 mM)	0.08, 0.1
		750 (0.02 mM)	0.1
P87Stop		20,000 (0.07 mM)	2
BNP-II		20,000 (0.2 mM)	1.0
		7,900 (0.02 mM)	1.0
Des-1–6, BNP-II		12,000 (0.01 mM)	2
Des-1–6,des-87–95 BNP-II		60,000 (0.1 mM)	4

The binding and non-binding fractions were distinguishable electrophoretically; the binding fraction moved ~5% more rapidly to the anode than the non-binding fraction, suggesting tighter folding. It is significant that no component with the same mobility as the binding fraction was identifiable in the non-binding fraction, indicating that the binding affinity of the folded protein, while possibly not normal, was not reduced to an extent that prevented complete retention by the column. Although only very small quantities of binding protein could be isolated, the differences in folding between binding-competent and binding-incompetent protein were discernible in NMR spectra (see below) and in disulfide CD spectra, the CD spectrum of the non-binding component, as other non-binding components, completely lacking the 245-nm positive CD band (data

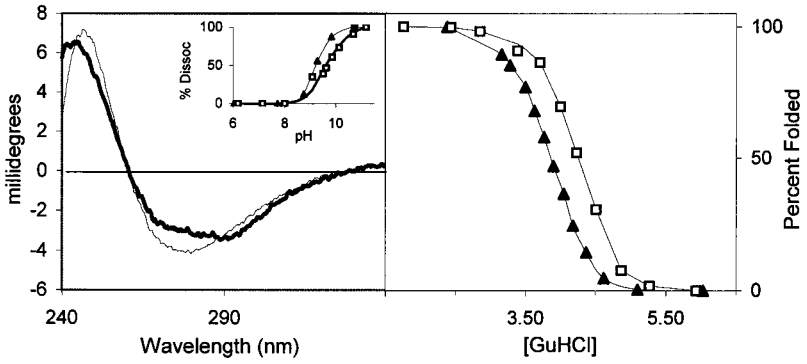

FIG. 5. **Relative stabilities of the WT and G57S precursors as monitored by the effects of pH and guanidine HCl.** *Left,* near-ultraviolet CD spectrum of the G57S precursor at neutral pH (*bold line*) and at pH 11. The change in this region is assigned to the dissociation of internal NP-hormone interactions (20). *Inset,* plot of the % dissociation of the internal complex as a function of pH, as calculated from the 280/291-nm ellipticity ratio for the WT protein (□) and G57S mutant (▲). *Right,* plot of % unfolding at pH 6 as a function of guanidine HCl concentration (*[GuHCl]*) for the WT and G57S precursors; *symbols* are the same as in the *inset.*

not shown). However, CD spectra of the binding fraction were also clearly atypical (Fig. 6). The intensity of the 245-nm positive peak characteristic of the folded state relative to that of the 280-nm negative band was markedly lower than in the WT protein, and this difference was increased at low pH. Note that the intensity of this peak in the WT protein is essentially independent of pH (*e.g.* Ref. 31). With the assumption that the disulfides are correctly paired in the binding fraction, the results indicate that, even with the correct pairing, mutation of Gly-17 to Val alters the folded state.

Fig. 7 compares regions of the proton NMR spectra of the non-binding form of the G17V mutant with that of the folded WT protein at pH 6.2. The region downfield of 4.7 ppm contains aromatic protons and α-protons that are downfield-shifted by β-sheet formation; the peak at 6.7–6.8 ppm represents the 3,5 ring protons of Tyr-49 and can be used as an intensity reference (26). The results show the presence in the non-binding form of the G17V mutant of a diminished number of downfield-shifted α-protons relative to WT, suggesting a significant reduction in β-structure, *e.g.* note the complete absence of a 6.2- or 6.4-ppm signal. Quantities of the binding form of G17V were inadequate for good spectra, but signals throughout the spectrum show its greater similarity to WT than to the G17V non-binding species; particularly note the 1.7-ppm region (Fig. 7).

Two other studies of the 14–18 turn were carried out. We particularly wanted to learn whether β-sheet formation forced formation of the turn, which was sterically hindered by a Val in position 17, or whether the turn actively promoted the docking of β-strands. In one study, native BNP-I was treated with Lys-C protease to generate an internal clip after Lys-18 (see "Materials and Methods"). Previous studies (26) had demonstrated that insertion of an internal clip after Glu-47 in native NP did not significantly alter conformation. If the turn played only a passive role, its cleavage after the correct disulfides were formed should also not significantly alter conformation. In the case of cleavage after Lys-18, however, all the protein became binding-incompetent, and the 245-nm positive CD band was completely lost (data not shown). Significantly, the NMR spectrum of this derivative (Fig. 7) was almost identical to that of the non-binding component of the G17V mutant, consistent with a similar effect on β-structure.

We also investigated the effect of expanding the size of the 14–18 turn by interposing the sequence AG between Gly-17 and Lys-18. With the exception of a greater (but still low) folding efficiency (see "Materials and Methods"), the folding properties of the mutant (turn AG) were analogous to those of the G17V mutant. As with the G17V mutant, additional folded protein could be formed from the binding-incompetent fraction

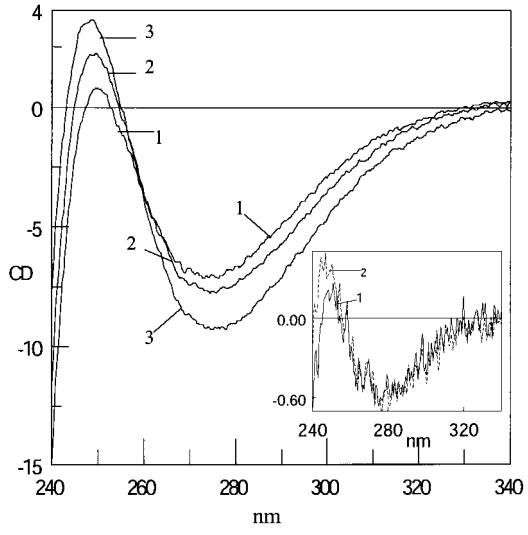

FIG. 6. **Near-ultraviolet CD spectra of binding-competent Gly-17 turn mutants as a function of pH.** *Inset,* G17V at pH 2.1 (*curve 1*) and pH 6.2 (*curve 2*). *Main figure,* turn AG mutant at pH 2.5 (*curve 1*), pH 3 (*curve 2*), and pH 6.2 (*curve 3*). CD data are expressed in millidegrees ellipticity.

by resubjecting it to folding conditions. In this case, we additionally demonstrated that this was not the case if β-mercaptoethanol was omitted during refolding, showing that disulfide rearrangement was critical to the refolding process.

Analysis of the turn AG binding fraction by CD indicated spectral properties similar to those of G17V (Fig. 6). The 245-nm positive band was barely evident at pH 2.5 but increased in intensity with an increase in pH to 6.2, although it did not achieve the intensity of the WT protein under these conditions. Preliminary CD studies in the far UV suggested a lower content of β-sheet in that mutant than in the WT protein. Native BNP-I and -II have atypical CD spectra in this region for proteins rich in β-sheet (*e.g.* Refs. 22 and 29), with a single negative band at 208–209 nm that shifts to 203–204 nm on denaturation (*e.g.* Ref. 29). The turn AG mutant exhibited a negative band centered at ~204 nm and did not achieve the positive ellipticity in the 190–200-nm region seen for the folded WT protein. We assume that the binding-competent G17V and turn AG mutants have the correct disulfide pairs. Nonetheless, the optical activity of these mutants indicates that their conformations differ from that of the folded WT protein.

Effects of Deletion of Glu-47—Glu-47 plays a central role in binding the hormone α-amino group, the latter thus far critical

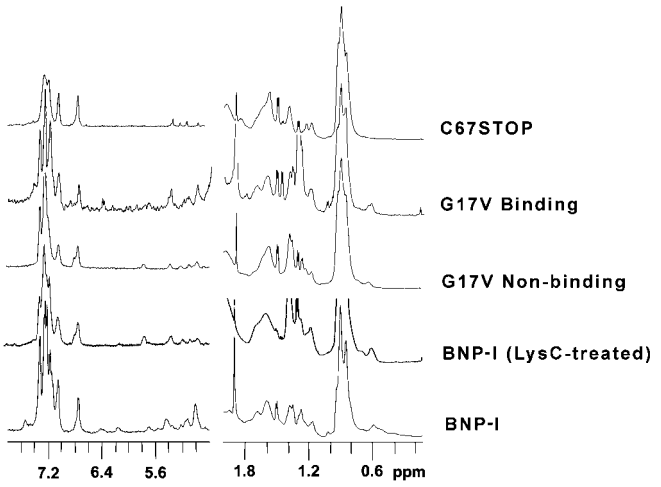

FIG. 7. **Proton NMR spectra of selected binding-competent and binding-incompetent species in D_2O at pH 6.2.** From *top* to *bottom*: C67STOP, 0.4 mM; G17V, binding-competent, concentration unknown; G17V, binding-incompetent, 0.3 mM; BNP-I, Lys-C protease-treated, 0.8 mM; BNP-I (native), 0.3 mM. See Fig. 4 for other details.

to recognition by NP (2). Its deletion also alters the 3,10 helix. Accordingly, no binding-competent protein was isolated from the ΔE47 mutant, and the presence of peptide during folding had no clear influence on the final product. However, fractionation of the binding-incompetent protein by HPLC (see "Materials and Methods") led to isolation of a discrete component with a strong positive CD band at 245 nm (Fig. 3). The 245/280 nm ratio for this peak was 60% that of the WT protein and has so far not been improved by refractionation. The yield of this component was approximately half that of the WT protein (see "Materials and Methods").

Folding of the HPLC-purified protein was confirmed by NMR. The spectrum of this component (Fig. 4) suggested β-sheet formation similar, but not necessarily identical, to that of WT protein, as evidenced particularly by the chemical shifts and content of downfield α-protons. Signals at ~6.2 and ~6.4 ppm associated with monomer and dimer, respectively, in the native protein are slightly shifted in the mutant but were demonstrated to be similarly affected by changes in dimerization induced by changes in concentration or pH. Assuming that the fractionated protein is homogeneous, the dimerization constant calculated from the relative intensity of these signals is essentially identical to that of the WT protein in D_2O alone (Table II). However, we cannot exclude the possibility that the low 245/280 nm ratio reflects the presence of unfolded protein that was not separated from folded protein by HPLC. Since such protein can be maximally estimated as ~50% in content (this assumes a normal 245/280 nm ratio for the folded Glu-47 deletion mutant and typical spectral properties (29) for the unfolded protein) and should neither dimerize nor contribute to signals at 6.2 and 6.4 ppm, the actual dimerization constant might be twice as high as that shown. The stability of the mutant was within experimental error of that of the WT protein (Table III).

Although the hormone (or peptide) α-amino group has always appeared essential to binding to NP, it binds to groups additional to Glu-47 (6, 7). Accordingly, we looked for peptide binding by the ΔG47 mutant that would be too weak to allow its interactions with the affinity support. CD binding studies using the mononitrated form of the protein (see "Materials and Methods") indicated no perturbation of the protein nitrotyrosine at concentrations of Phe-Tyr-NH_2 as high as 28 mM, but the nitrotyrosine appeared optically inactive in this mutant. We then investigated the effect of peptide (Phe-PheNH_2) on the NMR spectrum of the (non-nitrated) mutant. Small changes were reproducibly seen in the intensity ratio of the dimer and monomer signals at ~6.4 and 6.2 ppm, which were not assignable to signals from the free peptide and which suggested an increase in dimerization constant in the presence of peptide (data not shown). However, these changes were unaccompanied by other changes normally associated with increased dimerization and require additional investigation.

Effects of Termination of NP at Residue 66—Essentially all of the peptide-binding site on NP resides within the first 60 residues (6, 7). Nonetheless, no demonstrable binding-competent protein was obtained from folding mixtures of the C67STOP mutant (see "Materials and Methods"). The binding-incompetent protein gave a near-UV circular dichroism spectrum (Fig. 3) similar in shape, but weaker in 280-nm negative molar intensity, to that typical of binding-incompetent protein. Because the incomplete set of disulfides present might itself lead to an altered spectrum, an NMR spectrum was also obtained (Fig. 7). Several relatively weak downfield-shifted α-protons were seen, suggestive of β-sheet. The intensity of these signals relative to the 2-proton signal from Tyr-49 at ~6.8 ppm allows the presence of ~30% of a species with partial β-structure content, if all belong to the same component. However, in contrast to the ΔE47 mutant, reverse phase HPLC analysis failed to resolve discrete components of the C67STOP mutant, the protein migrating as a single very diffuse band (see "Materials and Methods"). Far ultraviolet CD analysis of different sections of this band revealed only subtle differences that were not amenable to interpretation, and all the spectra generally resembled that of unfolded NP.

Effects of Termination of NP at Residue 86—The yield of folded protein obtained from the P87STOP mutant (see "Materials and Methods") and its near UV circular dichroism spectrum (Fig. 3) and stability (Table I) were essentially the same as those of the WT protein. Apart from the loss of signals from the deleted carboxyl-terminal residues, proton NMR spectra (Fig. 4) were also normal for folded NP. However, the peptide binding constant of the 87STOP mutant was twice that of the WT protein at the same protein concentration (Table III), whereas the dimerization constant was only half that of the WT protein (Table II). The results signify a higher intrinsic binding constant to the monomeric and/or dimeric mutant protein than to the WT protein; as with the WT protein, NMR spectra indicated that addition of peptide to the P87STOP mutant converted the equilibrium mixture of monomer and dimer to all dimer, the data indicating a minimum 100-fold increase in dimerization constant in the presence of ligand (Fig. 4).

Because these results did not provide clear evidence of a defect that might contribute to diabetes insipidus (see "Discussion"), and because the conditions used to fold the protein during preparation are not sensitive to minor folding defects (see "Materials and Methods"), we also compared the rate of folding of the completely reduced protein with that of the WT protein under identical conditions, using procedures described earlier for studies of folding kinetics (16). The rate of folding of the P87STOP mutant was within experimental error of that of the WT protein (Fig. 8), arguing that deletion of the carboxyl terminus does not negatively impact on folding mechanism. It is further relevant that the first order folding rate constant of both proteins ($7 \pm 1 \times 10^{-3}$/min) was almost three times the value of 2.4×10^{-3}/min obtained for WT bovine NP-II under identical conditions (16); this difference paralleled the greater stability of the folded state of BNP-I than of BNP-II relative to their guanidine-denatured states (Table I) or to their disulfide-

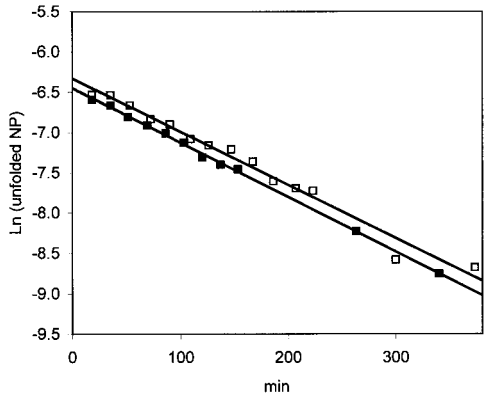

FIG. 8. **First order refolding plots of WT BNP-I (□) and the P87 STOP mutant (■) from the reduced state.** Rates were monitored as described previously (16) at pH 7.3 in a redox buffer containing 2 mM GSH, 2 mM GSSG, and 10 mM Phe-Tyr-NH_2. The calculated first order rate constants are 6.8×10^{-3} and 6.6×10^{-3}/min for the P87STOP and WT proteins, respectively.

mispaired states (20).[3] The similarity of folding rates and of stabilities to guanidine denaturation (Table I) of BNP-I and the P87STOP mutant therefore also strongly suggest similar stabilities relative to their disulfide-mispaired states and the lack of importance of the 87–93 region to this property.

We also enzymatically prepared a derivative of BNP-II lacking residues 1–6 and 87–95 (see "Materials and Methods"), and we compared its properties with that of native BNP-II and with des-1–6 BNP-II. In this case, the peptide binding constant of the des-1–6,des-87–95 mutant was ~4× that of the WT protein at the same protein concentration (Table III). The binding constant of its parent des-1–6 protein could not be determined under the same conditions because of the insolubility of its complexes, but was only twice that of the WT protein at lower protein concentrations (Table III); thus half of the increase in binding by the des-1–6,des-87–95 protein appears to derive from deletion of residues 87–95. The dimerization constant of the des-1–6,des-87–95 protein was trivially higher than that of native BNP-II but was only 1/4 that of its parent des-1–6 protein (Table II). As with the P87STOP mutation, deletion of the carboxyl terminus therefore negatively impacted on dimerization but increased binding affinity. No clearly significant differences in stability between native BNP-II and either the des-1–6 protein or the des-1–6,des-87–95 protein were observed (Table I).

DISCUSSION

Implications for the Relationship between Neurophysin Structure and Properties—The sensitivity of folding to alterations in the Gly-17 turn and the loss of structure upon cleavage of this turn in the native folded protein are particularly striking. Modeling suggests that the destabilization associated with the G17V mutation arises principally from the energy barrier involved in fitting Val-17 ϕ and ψ angles (32) to the Gly-17 values (approximately +60 and +26 in the unbound state, respectively), with potential additional contributions from Val hydrophobicity. The instability arising from expansion of the turn by the AG insert probably in part involves other mechanisms, since such expansion should reduce the ϕ and ψ angle constraints needed to correctly position the loop ends and because Ala hydrophobicity is a lesser issue; note that the side chain of Lys-18, which immediately follows the insert, is not involved in any critical interactions in the folded structure. The Lys-C protease results are relevant here. Assuming that cleavage of the turn by Lys-C is not accompanied by disulfide rearrangement (see "Materials and Methods"), the conformational rearrangement associated with turn cleavage signifies that tethering of the ends of the β-strands is critical to β-strand docking in this case, perhaps because of the short length (3 residues) of one of the connected strands. It follows that the length and composition of the turn will play a central role in sheet alignment, in this case the increased flexibility associated with the AG insert reducing tethering efficiency.

The critical requirements for β-sheet docking in this system contrast with the lack of sensitivity of folding to changes in the 3,10 helix. Previous studies (26) demonstrated that this helix could be cleaved in folded NP without significant effect on either conformation or dimerization. The present results indicate that altering the helix by deletion of Glu-47 does not interfere with folding from the reduced state, except to the extent that the additional stabilization of the folded state induced by peptide binding and required for efficient folding is lost. The folding efficiency of the ΔE47 mutant, approximately half that of BNP-I in the presence of peptide, is consistent with what would be expected for BNP-I in the absence of peptide, given that the folded and disulfide-mispaired states of BNP-I are of approximately equal stability (*cf.* Refs. 16 and 20). Additionally, the structure of the folded state indicates a high content of β-sheet and at most only minor differences from unliganded BNP-I in dimerization; the results in general indicate a high degree of independence of global protein conformation from that of the helix.

We did not evaluate dimerization in the more severely folding-compromised mutants, but clear reductions in dimerization were evident in the G57S, G57R, and 87STOP mutants. The reductions in dimerization in the unliganded G57S and G57R mutants implicate a role for loop structure in the relative orientation of the two NP domains, both of which participate in dimerization (6, 7). This is similarly suggested by the effects on dimerization of succinylation of Ser-56. However, mutation of Gly-57 has so far not reduced ligand-facilitated dimerization, whereas succinylation of Ser-56 appears to block this process (25), suggesting that the Ser-56 modification has a greater effect than the Gly-57 mutations on dimerization in the liganded state.

In the case of the 87STOP mutant, the small decrease in dimerization constant is accompanied by an increased binding constant, and these effects are also seen upon deletion of residues 87–95 in BNP-II. The deleted region has not been seen in any BNP-II crystal structure (6, 7), but the structure of the unliganded state[2] places residue 86 within 8 Å of interface residues of the neighboring subunit, allowing the possibility that residues carboxyl-terminal to residue 86 might be in still closer proximity. Thus, the decrease in dimerization constant upon deletion of the carboxyl terminus, which represents ~0.4 kcal/mol in BNP-I and 0.8 kcal/mol in the case of the des-1–6 BNP-II, might reflect ancillary stabilizing interactions by carboxyl-terminal residues across the subunit interface. It is relevant that solution studies (*e.g.* Refs. 27 and 33) and crystal structure comparisons of liganded and unliganded states[2] indicate small ligand-induced changes in the subunit interface. Since the increase in binding constant upon deletion of the carboxyl terminus is similar energetically to the decrease in dimerization constant, the binding constant increase may reflect a decreased uphill energy requirement for ligand-induced interface alteration when carboxyl-terminal interactions are lost.

The mutation that had the most negative impact on folding was, not surprisingly, that of terminating the protein at resi-

[3] S. Eubanks, T. L. Nguyen, R. Deeb, A. Villafania, A. Alfadhli, and E. Breslow, unpublished observations.

due 66. This mutation deletes almost all of the carboxyl-terminal domain and necessarily leaves one Cys residue without a partner. We attribute the lack of folding both to the odd number of cysteines, which increases the opportunity for disulfide mispairing in this metastable disulfide-rich protein, and to the almost complete loss of the carboxyl domain, the noncovalent interactions of which with the amino domain appear to be necessary for stability. Thus, in preliminary studies, we have found that mutation of Cys-85 to Phe, which retains the carboxyl domain but leaves an unpaired Cys residue, and mutation of the codon for Cys-61 to a STOP, which completely deletes the carboxyl domain without leaving an unpaired Cys residue, are each associated with complete loss of folding. The C61STOP mutation is also associated with diabetes insipidus (9), providing further evidence that the amino domain is too unstable to fold efficiently without stabilization by the carboxyl domain.

Implications for the Etiology of Diabetes Insipidus—The intracellular accumulation of mutant vasopressin precursor in FNDI might in principle result from a failure to fold and consequently a failure to target to regulated neurosecretory granules, or a failure of properly folded protein to target because of a loss of some sequence or other attribute (such as the necessary self-association properties) required for targeting. In the present studies, all mutants except P87STOP exhibited defects that would, to varying extents, reduce folding efficiency. Additionally, the greater intrinsic stability of the folded state of bovine ^{Oxy}NP than of bovine ^{VP}NP and the stronger homology of human ^{VP}NP to bovine ^{VP}NP than to bovine ^{Oxy}NP (Fig. 1) suggest that these mutations have the potential to impact folding of the human vasopressin precursor more than seen here for bovine ^{Oxy}NP and its precursor.

The relative impact of the G17V, ΔE47, G57S, and C67STOP mutations on the trafficking and processing of the human vasopressin precursor in cell culture generally parallels the relative magnitude of their effects here on the properties of mature NP and their projected impact on the folding of the corresponding precursors. In order of their inhibitory effects on folding, our data indicate C67STOP > G17V > ΔE47 > G57S. This agrees with studies by Olias *et al.* (34) and Nijenhuis *et al.* (11) which indicated that the G17V mutant does not exit the ER (34) but that small quantities of G57S and, to a lesser extent, ΔE47 do exit the ER. It also agrees with studies by Ito *et al.* (35) who reported adverse effects of mutations on the secretion of the corresponding precursors in the order C67STOP > ΔE47 > G57S (35). Although G57S appears to adversely affect cell viability more than ΔE47 (10), the agreement between the biological and physical-chemical data is generally consistent with a model in which only the correctly folded human vasopressin precursor, with the ability to form normal dimers, has a significant ability to exit the ER. The finding that a fraction of the ΔE47 mutant exits the ER additionally allows the possibility that the increase in dimerization constant associated with ligand binding may not be required for efficient trafficking of the fraction that folds, although further studies of potential hormone-NP interactions within this precursor, and their impact on both folding and dimerization, are clearly needed. Note that some mutants have been shown to associate via disulfide formation, as opposed to the normal non-covalent mechanism, yielding dimers and higher oligomers that do not exit the ER (36). Such covalent self-association may account for the apparent ability of the C67STOP mutant to dimerize, suggested by cross-linking (35), since both our failure to find significant folding of this mutant and the absence of half of its interface argue that it is unlikely to dimerize by normal mechanisms.

Beyond this qualitative agreement between folding thermodynamics and pathogenicity for the above mutations, however, unanswered questions remain. Consider the G57S mutation. We find that this destabilizes the bovine oxytocin precursor by only ~0.6 kcal/mol, while cell culture studies indicate that secretion of arginine vasopressin immunoreactivity into cell culture media from precursors with this mutation is impaired by ~90% (11, 35). By using methods previously described to estimate precursor folding efficiency (20), a 0.6 kcal/mol destabilization is predicted to only reduce the theoretical folding efficiency of the bovine oxytocin precursor from 98 to 94% under ER conditions. Even allowing for a lower stability of the WT human vasopressin precursor than of the bovine oxytocin precursor, there is no mechanism based on folding thermodynamics alone by which a mutation-induced 0.6 kcal/mol further decrease in stability would reduce folding by 90%. One potential explanation lies in the response of the ER to the presence of misfolded protein (37), which may amplify the effect of a relatively small degree of misfolding, *e.g.* the presence of misfolded mutant precursor in the ER has been shown to impair the secretion of folded protein (35). Alternatively, the mutation may have a greater energetic impact on the human vasopressin precursor than on the bovine oxytocin precursor. We particularly note the possibility that direct or indirect interactions of the G57S mutation with copeptin, or with other elements of sequence of the human vasopressin precursor not found in the bovine oxytocin precursor, might be more destabilizing to the human protein.

The principal unanswered questions concern the 87STOP mutation. This is the sole mutation for which we find no clear parallel in a change in the physical properties of bovine NP. Recent cell culture studies (38) indicate that incorporation of this mutation into the human vasopressin precursor leads to a large fraction of it accumulating in the ER, suggesting a folding defect; the remainder appears to be normally handled. However, we find no evidence of a folding defect in the mature mutant, and no change is seen in other physical properties that might significantly impact on precursor stability. The small reduction in dimerization constant in the unliganded state that accompanies loss of the carboxyl terminus is accompanied by a compensating increase in binding affinity and the normal ligand-facilitated increase in dimerization. The stability of the mutant precursor should therefore be similar to that of the WT precursor unless factors unique to the human protein are involved. This possibility merits exploration. For example, modeling of the sequence differences between human and bovine ^{VP}NPs into the structure of BNP-II provocatively suggests very close proximity between the Phe substitution at position 70 of human NP (Fig. 1) and Arg-86.

Is it possible that the defect in the 87STOP mutant lies in a targeting defect that does not involve a folding defect? We tentatively discount decreased dimerization as causative in this case, since the high dimerization constant of the liganded state might provide essentially complete dimerization at ER protein concentrations. Similarly, deletion of the carboxyl-terminal glycopeptide has been reported to facilitate, not hinder, targeting (4). However, the potential role in targeting of human ^{VP}NP residues 87–93 (Fig. 1) remains to be evaluated. Additionally, in view of evidence for a role of protein insolubility in targeting to regulated secretory granules (14, 39) and the increased solubility of complexes of des-1–6 BNP-II upon cleavage of its carboxyl terminus (see "Results"), a role for the carboxyl terminus in higher order aggregation processes that might contribute to targeting is not implausible. Physical-chemical studies of the human vasopressin precursor and of its mutants are clearly needed to resolve these and other ambigu-

ities noted here and, in doing so, have the potential to increase understanding of the complex factors (14) involved in targeting to the regulated secretory pathway.

Acknowledgments—We thank Dr. Chandana Barat for conducting preliminary studies of the C85F and C61STOP mutants. We are particularly grateful to Dr. David Peyton for guiding NMR studies of the dimerization properties of the succinylated protein.

REFERENCES

1. Land, H., Schutz, G., Schmale, H and Richter, D. (1982) *Nature* **295,** 299–303
2. Breslow, E., and Burman, S. (1990) *Adv. Enzymol.* **63,** 1–67
3. Land, H., Grez, M., Ruppert, S., Schmale, H., Rehbein, M., Richter, D., and Schutz, G. (1983) *Nature* **302,** 342–344
4. Kim, J. K., Summer, S. N., Wood, W. M., Brown, J. L., and Schrier, R. W. (1997) *J. Am. Soc. Nephrol.* **8,** 1863–1869
5. Ando, S., McPhie, P., and Chaiken, I. M. (1987) *J. Biol. Chem.* **262,** 12962–12969
6. Chen, L., Rose, J. P., Breslow, E., Yang, D., Chang, W. R., Furey, W. F., Jr., Sax, M., and Wang, B.-C. (1991) *Proc. Natl. Acad. Sci. U. S. A.* **88,** 4240–4244
7. Rose, J. P., Wu, C. K., Hsaio, C. D., Breslow, E., and Wang, B.-C. (1996) *Nat. Struct. Biol.* **3,** 163–169
8. Ito, M., Mori, Y., Oiso, Y., and Saito, H. (1991) *J. Clin. Invest.* **87,** 725–728
9. Rittig, S., Robertson, G. L., Siggaard, C., Kovacs, L., Gregersen, N., Nyborg, J., and Pedersen, E. B. (1996) *Am. J. Hum. Genet.* **58,** 107–117
10. Ito, M., Jameson, L., and Ito, M. (1997) *J. Clin. Invest.* **99,** 1897–1905
11. Nijenhuis, M., Zalm, R., and Burbach, J. P. H. (1999) *J. Biol. Chem.* **274,** 21200–21208
12. Breslow, E. (1993) *Regul. Pept.* **45,** 15–19
13. de Bree, F. M., and Burbach, J. P. (1998) *Cell. Mol. Neurobiol.* **18,** 173–191
14. Arvan, P., and Castle, D. (1998) *Biochem. J.* **332,** 593–610
15. Nicolas, P., Batelier, G., Rholam, M., and Cohen, P. (1980) *Biochemistry* **19,** 3565–3573
16. Deeb, R., and Breslow, E. (1996) *Biochemistry* **35,** 864–873
17. Eubanks, S., Nguyen, T., Peyton, D., and Breslow, E. (2000) *Biochemistry* **39,** 8085–8094
18. Bahnsen, U., Oosting, P., Swaab, D., Nahke, P., Richter, D., and Schmale, H. (1992) *EMBO J.* **11,** 19–23
19. Chauvet, M. T., Hurpet, D., Chauvet, J., and Acher, R. (1983) *Proc. Natl. Acad. Sci. U. S. A.* **80,** 2839–2843
20. Eubanks, S., Lu, M., Peyton, D., and Breslow, E. (1999) *Biochemistry* **38,** 13530–13541
21. Huang, H.-B., and Breslow, E. (1992) *J. Biol. Chem.* **267,** 6750–6756
22. Breslow, E., Aanning, H. L., Abrash, L., and Schmir, M. (1971) *J. Biol. Chem.* **246,** 5179–5188
23. Virmani-Sardana, V., and Breslow, E. (1983) *Int. J. Pept. Protein Res.* **21,** 182–189
24. Rabbani, L., Pagnozzi, M., Chang, P., and Breslow, E. (1982) *Biochemistry* **21,** 817–826
25. Huang, H.-B., LaBorde, T., and Breslow, E. (1993) *Biochemistry* **32,** 10743–10749
26. Zheng, C., Peyton, D., and Breslow, E. (1997) *J. Pept. Res.* **50,** 199–209
27. Breslow, E., LaBorde, T., Bamezai, S., and Scarlata, S. (1991) *Biochemistry* **30,** 7990–8000
28. Coligan, J. E., Dunn, B. M.,. Ploegh, H. L., Speicher, D. W., and Wingfield, P. T. (eds) (1995) *Current Protocols in Protein Science,* Vol. 2, A.3A.1–A.3A.4, John Wiley & Sons, Inc., New York
29. Menendez-Botet, C. J., and Breslow, E. (1975) *Biochemistry* **14,** 3825–3835
30. Kanmera, T., and Chaiken, I. M. (1985) *J. Biol. Chem.* **4,** 8474–8482
31. Breslow, E., and Gargiulo, P. (1977) *Biochemistry* **16,** 3397–3406
32. Walther, D., and Cohen, F. E. (1999) *Acta Crystallogr. Sect. D Biol. Crystallogr.* **55,** 506–517
33. Breslow, E., Sardana, V., Deeb, R., Barbar, E., and Peyton, D. H. (1995) *Biochemistry* **34,** 2137–2147
34. Olias, G., Richter, D., and Schmale, H. (1996) *DNA Cell Biol.* **15,** 929–935
35. Ito, M., Yu, R. N., Jameson, L., and Ito, M. (1999) *J. Biol. Chem.* **274,** 9029–9037
36. Beuret, N., Rutishauser, J., Bider, M. D., and Spiess, M. (1999) *J. Biol. Chem.* **274,** 18965–18972
37. Harding, H. P., Zhang, Y., Bertolotti, A., Zeng, J., and Ron, D. (2000) *Mol. Cell* **5,** 897–904
38. Nijenhuis, M., Zalm, R., and Burbach, J. P. (2000) *Mol. Cell. Endocrinol.* **167,** 55–67
39. Chanat, E., and Huttner, W. B. (1991) *J. Cell Biol.* **115,** 1505–1520
40. Pace, C. N. (1975) *Crit. Rev. Biochem.* **3,** 1–43

Effects of Diabetes Insipidus Mutations on Neurophysin Folding and Function

Sharon Eubanks, Tam L. Nguyen, Ruba Deeb, Art Villafania, Ayna Alfadhli and Esther Breslow

J. Biol. Chem. 2001, 276:29671-29680.
doi: 10.1074/jbc.M103477200 originally published online June 6, 2001
